Physiological
Measurement

PAPER • OPEN ACCESS

Dissecting the integrated information of cardiovascular and cardiorespiratory systems at rest and during physiological stress

To cite this article: Irene Franzone *et al* 2026 *Physiol. Meas.* **47** 075001

IOP Publishing Physiol. Meas. 47 (2026) 075001 https://doi.org/10.1088/1361-6579/ae7fec

Physiological Measurement

IPEM Institute of Physics and Engineering in Medicine

Check for updates

OPEN ACCESS

RECEIVED
5 March 2026

REVISED
17 June 2026

ACCEPTED FOR PUBLICATION
19 June 2026

PUBLISHED
6 July 2026

PAPER

Dissecting the integrated information of cardiovascular and cardiorespiratory systems at rest and during physiological stress

Irene Franzone[1], Roberta Saputo[1], Yuri Antonacci[1], Michal Javorka[2], Riccardo Pernice[1,*] and Luca Faes[1,3]

1 Department of Engineering, University of Palermo, Palermo, Italy
2 Department of Physiology, Jessenius Faculty of Medicine in Martin, Comenius University in Bratislava, Martin, Slovakia
3 Faculty of Technical Sciences, University of Novi Sad, Novi Sad, Serbia
* Author to whom any correspondence should be addressed.

E-mail: riccardo.pernice@unipa.it

Keywords: integrated information theory, causal density, whole-minus-sum integrated information, information dynamics, cardiovascular system, cardiorespiratory system, physiological stress

Abstract

Objective. In the framework of integrated information theory, different measures have been proposed to quantify the information integrated in a dynamic system composed by interconnected units, each capturing a different aspect of the system connections. While integrated information measures have been traditionally applied to brain dynamics, in this study we propose their implementation for the investigation of the short-term regulation of cardiovascular (CV) and cardiorespiratory (CR) systems reflected by the spontaneous variability of heart period (HP), systolic arterial pressure (SAP) and respiration (RESP). *Approach.* We selected two integrated information measures related to well-known dynamic properties of CV and CR systems: whole-minus-sum (WMS) quantifying the information stored in the whole system above and beyond the information stored in its units, and causal density (CD) that handles integration in terms of the information transferred between the system units. WMS and CD measures were computed from the parameters of vector autoregressive models fitted respectively on the bivariate time series of {HP, SAP} and {HP, RESP}, obtained from healthy young subjects at rest, during head-up tilt and during a mental arithmetic task. *Main results.* We found that CV and CR systems dynamically integrate significant amounts of information, which undergo modulations in response to the tasks performed, especially during tilt, proving that orthostatic stress significantly reduces the degree of cooperation between the parts of the systems. A different response to stress was observed for CD and WMS measures, related to the changes in the information storage and transfer induced by the orthostatic and mental challenges and their physiological interpretation. *Significance.* The possibility offered by the integrated information measures, in combination with their constituent contributions, allowed us to disentangle in a comprehensive way the statistical relationships underlying the CV and CR dynamics, and to investigate for the first time the concept of integration in the CV and CR systems.

1. Introduction

Physiological systems exhibit complex behavior arising from the combined effects of regulatory mechanisms, coupling, and feedback among structural units, with their dynamics shaped by various physiological and pathological states (Valente *et al* 2018). This behavior occurs for instance in the cardiovascular (CV) and cardiorespiratory (CR) systems, and results from the interaction among sub-systems cooperating to maintain homeostatic physiological activities. The activities of those systems, typically characterized through time series of the beat-to-beat variability of the heart period (HP), systolic arterial pressure (SAP) and respiration (RESP), are indeed of great physiological relevance (Cohen and Taylor 2002, Eckberg 2003). CV interactions are the result of a closed-loop composed of a negative feedback on

HP acting in response to SAP variation to maintain arterial pressure at a preset level (baroreflex), and a feed-forward effect of HP on SAP variability, which occurs as a consequence of changes in ventricular filling and diastolic runoff (Mullen *et al* 1997, Cohen and Taylor 2002). CR interactions, on the other side, encompass the effects of RESP on HP length, known as respiratory sinus arrhythmia (RSA), and an often ignored opposite interaction from HP to RESP resulting on cardioventilatory coupling (Galletly and Larsen 1998, Rosenblum *et al* 1998). In recent years, several methods for linear and nonlinear time series analysis have been proposed to characterize CV and CR dynamics, with the aim of disentangling physiological mechanisms from the spontaneous variability of HP, SAP, and RESP (Pompe *et al* 1998, Porta *et al* 2011, Schulz *et al* 2013). Although the analysis of individual systems provided helpful markers for the characterization of several physiological and pathological states, accumulating evidence highlighted the importance of studying distinct physiological systems within an integrated network perspective, where each system, despite having its own regulatory mechanisms, continuously interacts with many others (Ivanov 2021).

One aspect of understanding and controlling these systems is knowing how to describe and quantify the dynamical interactions that characterize their complex behavior. A common intuition is that dynamical complexity consists in the coexistence of differentiation (when the parts of a system behave as functionally distinct units) and integration (when the system, as a whole, exhibits functional coherence) in the dynamic evolution of the system at hand (Barrett and Seth 2011). Integrated information theory (IIT) is rooted in this frame, and was originally conceived in theoretical neuroscience to explain the origins and fundamental nature of consciousness (Tononi and Koch 2015). It constitutes a prominent theory that provides a mathematical approach to quantify the information integrated in the brain, the so called integrated information (Balduzzi and Tononi 2008, Tononi 2012). In its original formulation, referred to as 'strong IIT', the theory was found to be divisive because of its high claims (Mediano *et al* 2022). On the other hand, following a more pragmatic perspective, 'weak IIT' was proposed as a potential unifying framework to study complexity in general multivariate systems (Mediano *et al* 2022). Quite surprisingly, while this framework is widely adopted in neuroscience, it lacks applications in the field of computational physiology in spite of its expected usefulness (Hunter and Nielsen 2005).

In general, a measure of integrated information should capture and quantify the extent to which the dynamics of a multi-unit system are simultaneously differentiated and integrated (Seth *et al* 2011), where 'integration' can be understood as the degree of causal influences among elements (Oizumi *et al* 2016). Since this concept can be formalized in many different ways, a whole range of distinct integrated information measures have been advanced in the literature (Mediano *et al* 2018). In this work, we focus on two measures extensively used to characterize the dynamical behavior of complex systems, i.e. whole-minus-sum (WMS) integrated information and causal density (CD) (Seth *et al* 2011). WMS and CD measures reflect in different ways the extent to which the dynamics of a network system behave, providing insight on the amount of differentiation and integration of the system units. These measures are well-defined for stochastic systems and have the advantage that they can be estimated and interpreted starting from entropy-based measures like the predictive information (PI), the information storage (IS) and the transfer entropy (TE). PI and IS quantify the degree of predictability of the present state of a system given its own past states (Bialek *et al* 2001, Faes *et al* 2025), while TE quantifies the amount of information transfer from one stochastic process to another (Schreiber 2000). These measures have been recognized as powerful tools to assess dynamic systems, especially in networks of CV and CR interactions (Porta *et al* 2011, Faes *et al* 2017, 2025).

In this work, the WMS and CD measures of integrated information are applied for the first time to characterize the degree of integration of the CV and CR dynamic systems underlying the short-term regulation of the human heart rate in relation to the variability of arterial pressure and respiration. The purpose of the study is to introduce in the analysis of CV and CR dynamics the concept of integration operationalized through the WMS and CD measures, and to relate it to concepts commonly studied in this field such as those of regularity and causality of CV and CR oscillations, typically assessed through measures of PI and information transfer (Faes *et al* 2016). To this end, we show that the measures of WMS and CD can be dissected into quantities expressed in terms of PI/IS and of TE, respectively, and can be computed with high computational reliability from bivariate autoregressive (AR) models and their restricted univariate models (Mijatovic *et al* 2025). The analysis is performed on the spontaneous beat-to-beat variability series of HP, SAP and RESP measured in a large group of young healthy subjects monitored in a resting state and during conditions of head-up tilt and mental stress. The aim is to investigate how CV and CR systems integrate information in supine position and how their dynamic integration changes with postural and mental stress.

2. Materials and methods

2.1. Integrated information measures

2.1.1. Definitions and properties

Let us consider a bivariate dynamic system $\mathcal{S}$ composed of two possibly interacting units $\mathcal{X}$ and $\mathcal{Y}$, with dynamical activity described by the stationary vector random process $S_n = \{X_n, Y_n\}_{n\in\mathbb{Z}}$. Assuming S as a Markov process of order p, we denote as X_n and Y_n the random variables sampling the processes X and Y at the current time n, and as $X_{<n} = [X_{n-1}, \ldots, X_{n-p}]$ and $Y_{<n} = [Y_{n-1}, \ldots, Y_{n-p}]$ the variables describing the past history of the processes until lag p. With this notation, the total amount of Shannon information that is transferred over time through the analyzed processes can be quantified by the PI between the present and past states of the entire joint process S, denoted as (Faes *et al* 2025):

$$\begin{aligned} P_{X;Y} &= I(X_n, Y_n; X_{<n}, Y_{<n}) \\ &= H(X_n, Y_n) - H(X_n, Y_n | X_{<n}, Y_{<n}), \end{aligned} \tag{1}$$

where $H(\cdot)$, $H(\cdot|\cdot)$ and $I(\cdot)$ respectively represent entropy, conditional entropy and mutual information (Cover 1999). The PI, schematized in figure 1(a) in terms of Venn diagrams, quantifies the degree of predictability of the present state of the whole system given its own past states. It represents an extension to multivariate processes of the IS of a scalar process (Lizier *et al* 2014):

$$\begin{aligned} S_X &= I(X_n; X_{<n}) \\ &= H(X_n) - H(X_n|X_{<n}). \end{aligned} \tag{2}$$

The PI ranges from zero to the entropy of the system's present state, reflecting the regularity of the bivariate process arising from causal effects of the past states on the present one. Since the PI defined as in (1) cannot disentangle the causal sources giving rise to the flow of information over time, it can be decomposed evidencing quantities measuring the information stored within each individual system and the information transferred from one system to the other (Faes *et al* 2017). These quantities are the IS (2) and the information transfer quantified by the TE defined as (Schreiber 2000):

$$\begin{aligned} T_{X\to Y} &= I(Y_n; X_{<n} | Y_{<n}) \\ &= H(Y_n|Y_{<n}) - H(Y_n|X_{<n}, Y_{<n}), \end{aligned} \tag{3}$$

measuring the Granger-causal influence exerted over the present state of Y by the past states of X above and beyond the influence ascribed to the past states of Y itself.

IS and TE, as defined above, have been examined in previous research as components of the PI relevant about one individual target process (Faes *et al* 2017). Here, we consider how these measures can be interpreted as constituent terms of two well-known measures of integrated information. The first of these measures is the so-called CD (Seth *et al* 2011), which quantifies the average causal interactivity sustained by a system. CD, which was originally defined in terms of Granger causality (Seth *et al* 2011), can be rewritten in terms of TE exploiting the known link between GC and TE holding for Gaussian random processes (Barnett *et al* 2009). Then, for a bivariate process $\{X, Y\}$, the CD is simply defined as the mean of the TEs computed along the two directions of interaction from X to Y and from Y to X (Oizumi *et al* 2016):

$$\begin{aligned} \chi_{X;Y} &= \frac{1}{2}(T_{X\to Y} + T_{Y\to X}) \\ &= \frac{1}{2}(I(Y_n; X_{<n}|Y_{<n}) + I(X_n; Y_{<n}|X_{<n})). \end{aligned} \tag{4}$$

CD provides a measure of integrated information related to GC and dynamical complexity (Seth *et al* 2011): it is upper bounded by the PI (Mediano *et al* 2018), and it vanishes both for purely segregated systems where the parts are completely independent ($X \perp Y$) and for purely integrated systems when the parts are fully self-predictable ($S_X = H(X_n)$, $S_Y = H(Y_n)$); both conditions imply $H(X_n|X_{<n}) = H(X_n|X_{<n}, Y_{<n})$ and $H(Y_n|Y_{<n}) = H(Y_n|X_{<n}, Y_{<n})$, determining $\chi_{X;Y} = 0$. Therefore, according to the definition (4), a bivariate system exhibits integration when its elements exchange dynamically causal information and behave somewhat differently from each other. The Venn diagram representation of the CD related to the sum of two TE terms is reported in figure 1(b).

Another popular measure of integrated information is the so-called WMS integrated information, which quantifies the amount of information that is generated by the entire system beyond the information generated independently by its components (Oizumi *et al* 2016). When the system is constituted by

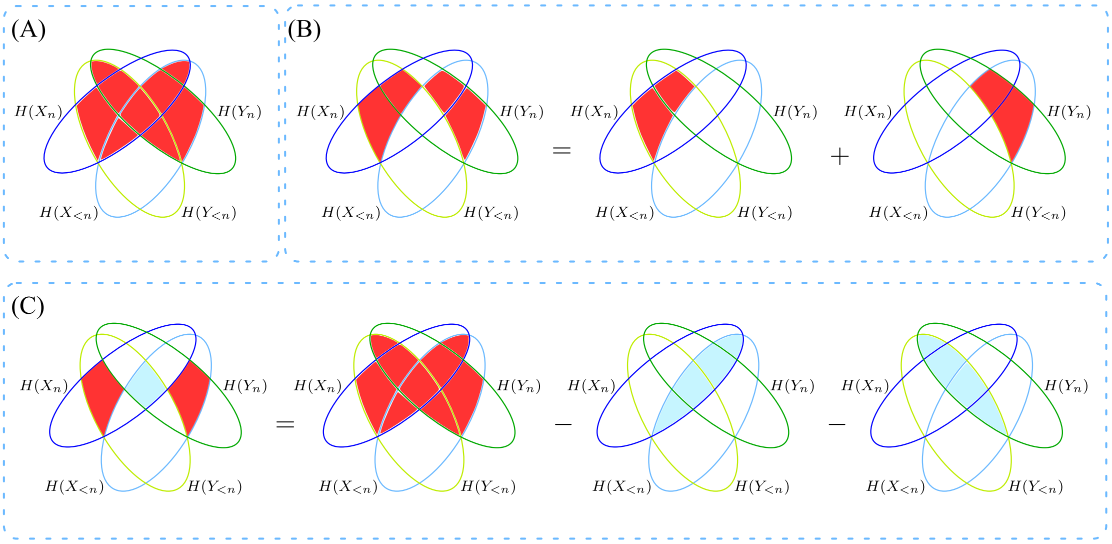

Figure 1. Venn diagrams depicting how the entropies of the present states ($H(X_n)$,$H(Y_n)$) and of the past states ($H(X_{<n})$,$H(Y_{<n})$) of two stationary random processes X and Y can be dissected to obtain: (A) the predictive information $P_{X;Y}$; (B) twice the causal density, $2 \cdot \chi_{X;Y}$, as the sum of transfer entropy $TE_{X\to Y}$ and $TE_{Y\to X}$; (C) the whole-minus-sum integrated information $\Phi_{X;Y}$ as the difference between predictive information $P_{X;Y}$, and information storage S_X, S_Y. In the diagrams, summed and subtracted information amounts are depicted in red and light blue, respectively.

two parts, the WMS measure is obtained taking the difference between the PI of the overall bivariate process $\{X, Y\}$ and the sum of the information stored in X and in Y:

$$\begin{aligned}\Phi_{X;Y} &= P_{X;Y} - S_X - S_Y \\ &= I(X_n, Y_n; X_{<n}, Y_{<n}) - I(X_n; X_{<n}) - I(Y_n; Y_{<n}).\end{aligned} \tag{5}$$

Equation (5) provides a measure of integrated information related to how good the system taken as a whole is in predicting its own evolution above and beyond its parts assessed in isolation. Like the CD, the WMS integrated information is upper bounded by the PI (Mediano *et al* 2018), and takes null values when the parts are independent ($X \perp Y$). However, its lower bound is not zero, because it quantifies also redundant contributions to the PI, i.e. contributions equally provided by $X_{<n}$ and $Y_{<n}$ to $\{X_n, Y_n\}$ (Mediano *et al* 2025); for example, when the units have undistinguishable dynamics ($X = Y$) all the terms of (5) are the same and the WMS integrated information becomes $\Phi_{X;Y} = -S_X = -S_Y$. Therefore, according to (5) a bivariate system exhibits integration when it stores more information than that stored individually by its parts, but it can also store less information than its parts. The Venn diagram representation of the WMS integrated information related to the PI of the whole system and the IS of its parts is reported in figure 1(c).

2.1.2. Practical computation

In the following, we provide the derivation of the integration measures $\chi_{X;Y}$ and $\Phi_{X;Y}$, as well as of their components related to TE and IS, under the assumption that the observed bivariate process has a joint Gaussian distribution. For a bivariate zero-mean jointly Gaussian process $S = \{X, Y\}$, the statistical dependencies between the present and past variables can be fully accounted by its vector AR representation (Barrett *et al* 2010):

$$S_n = \sum_{k=1}^{p} \mathbf{A}_k S_{n-k} + U_n \tag{6}$$

where $\mathbf{A}_k$ is the 2×2 coefficient matrix describing the interaction at lag k and U_n is a bivariate process formed by white and uncorrelated noises U_X and U_Y, representing the prediction error of the full model; the statistical description of the noise process is fully given by its covariance matrix $\Sigma_U = \mathbb{E}[U_n U_n^\intercal]$. Given the full AR model (6), the dynamics of each of the two individual processes X and Y are captured by the restricted models:

$$
\begin{aligned}
X_n &= \sum_{k=1}^{q} B_k X_{n-k} + W_n \\
Y_n &= \sum_{k=1}^{q} C_k Y_{n-k} + V_n
\end{aligned}
\tag{7}
$$

where q is the order of the restricted model. The parameters of the restricted models, i.e. the coefficients B_k, C_k and the prediction error variances $\sigma_W^2 = \mathbb{E}[W_n W_n]$ and $\sigma_V^2 = \mathbb{E}[V_n V_n]$, can be derived from the parameters of the full model (6), $\mathbf{A}_k$ and Σ_U, through the procedure described in detail in Mijatovic *et al* (2025). This procedure involves two steps: (i) deriving the time-lagged covariance structure of the bivariate process S; and (ii) reorganizing such structure to relate it to the covariance of the analyzed sub-process. The step (i) exploits the fact that the covariance of S, $\Sigma_{S,k} = \mathbb{E}[S_n S_{n-k}^T]$, is related to the AR parameters via the well-known Yule–Walker equations (Lütkepohl 2013):

$$
\Sigma_{S,k} = \sum_{l=1}^{p} \mathbf{A}_l \Sigma_{S,k-l} + \delta_{k0}\Sigma_U \tag{8}
$$

where δ_{k0} is the Kronecher delta function. This equation can be solved using the discrete-time Lyapunov equation to find the covariance $\Sigma_{S,k}$ from the parameters $\mathbf{A}_k$ and Σ_U. The step (ii) of the estimation procedure consists in extracting, from the covariance matrices $\Sigma_{S,k}$ computed for each lag $k \in \{0, 1, \cdots, q\}$, the covariance elements relevant to the sub-process X and Y and then solving the Yule–Walker equations relevant to each restricted model to find the variance σ_W^2 and σ_V^2 of the restricted models (Mijatovic *et al* 2025).

After model identification, the entropy-based measures can be estimated directly from the covariances of the residuals of the restricted and full models (Faes *et al* 2025). Specifically, the PI of the whole system can be expressed as:

$$
P_{X;Y} = \frac{1}{2}\ln\frac{|\Sigma_S|}{|\Sigma_U|}, \tag{9}
$$

where $|\cdot|$ represents the matrix determinant, while the IS of each part can be expressed as:

$$
S_X = \frac{1}{2}\ln\frac{\sigma_X^2}{\sigma_W^2}, S_Y = \frac{1}{2}\ln\frac{\sigma_Y^2}{\sigma_V^2}. \tag{10}
$$

Moreover, the transfer entropies are related to the ratio between the prediction error variances of the full and restricted models:

$$
T_{X\to Y} = \frac{1}{2}\ln\frac{\sigma_V^2}{\sigma_{U_Y}^2}, T_{Y\to X} = \frac{1}{2}\ln\frac{\sigma_W^2}{\sigma_{U_X}^2}, \tag{11}
$$

where $\sigma_{U_Y}^2$ and $\sigma_{U_X}^2$ are the variances of the prediction errors U_Y and U_X relevant to the full model (6), i.e. the diagonal elements of Σ_U.

The procedure described above for computing PI, IS and TE has the main advantage of relying exclusively on the identification of the parameters of the full AR model (6), from which the restricted model parameters can be derived as described rather than by re-identifying the models from subsets of data. In this work, full AR model identification was accomplished by employing the ordinary least squares method, selecting the order p via the Bayesian information-theoretic criterion (Schwarz 1978), with maximum scanned model order equal to 12. The order of the restricted models was set to $q = 20$, in accordance with previous works (Faes *et al* 2025).

2.2. Application to physiological time series

2.2.1. Dataset description and time series extraction

The study involved 127 healthy young volunteers (75 females; age: 18.6 ± 3.3 years), all normotensive and with body mass index within the normal range (21.4 ± 2.2 kg m^{-2}). The population was sex-balanced to limit the influence of this confounding factor on the analysis. The study was performed in accordance with the Declaration of Helsinki and it was approved by the ethical committee of the Jessenius Faculty of Medicine, Comenius University of Bratislava, Martin, Slovakia. All subjects or their legal representatives for minors (i.e. age < 18 years) signed a written informed consent to join the

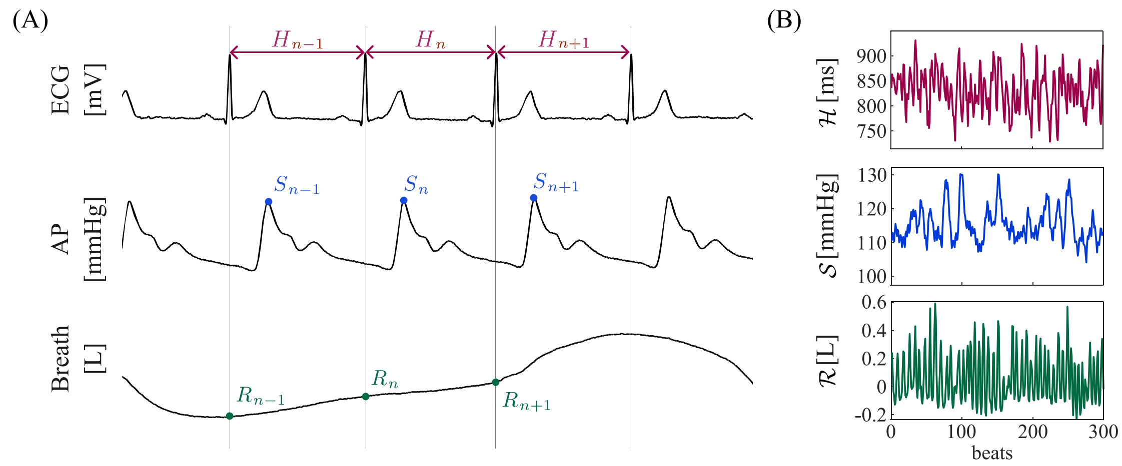

Figure 2. (A) Schematic representation of the measurement of beat-to-beat time series of heart period (H), systolic arterial pressure (S) and respiratory volume (R) from the recorded electrocardiographic (ECG), arterial pressure (AP) and respiratory volume (Breath) signals; (B) Time series of $\mathcal{H}$, $\mathcal{S}$ and $\mathcal{R}$ measured during REST for a representative subject.

experimental study. The experimental protocol consisted of three consecutive phases: (i) supine rest (REST, 15 min); (ii) head-up tilt (HUT), where each subject was tilted to 45 degrees for 8 min to evoke mild orthostatic stress; and iii) mental arithmetic task (MA) in the supine position for 6 min, where the subjects were instructed to sum up three-digit numbers (until one-digit number was reached) displayed on the ceiling of the examination room by a data projector and to decide if the final one-digit number was odd or even. During the MA task the subject was disturbed by the rhythmic sound of a metronome and instructed to perform the MA task as quickly as possible with a minimal error rate. During the entire procedure, the electrocardiogram (ECG; horizontal bipolar chest lead), arterial blood pressure (measured using the volume-clamp photoplethysmographic method), and respiratory volume signal (recorded via inductive plethysmography) were simultaneously acquired at a sampling rate of 1 kHz. From these signals, three time series were measured on a beat-to-beat basis: the nth HP (i.e. H_n) was computed as the time distance between the nth and the $(n+1)$th R peak of the ECG through the Pan-Tompkins algorithm (Pan and Tompkins 2007); the nth systolic AP value (i.e. S_n) was measured as the maximum of the AP waveform inside H_n; the nth RESP amplitude value (i.e. R_n) was computed sampling the respiratory volume signal on the nth R peak of the ECG. For each subject and experimental condition, time series of 300 heartbeats were selected according with international standards of short-term CV variability analysis (Shaffer and Ginsberg 2017). Before the analysis, to remove artifacts and favor the fulfillment of stationarity, the time series were high-pass filtered (IIR filter, cut-off frequency 0.0155 Hz) and reduced to zero mean. Stationarity of the pre-processed series was assessed both through visual inspection and by performing an Augmented Dickey–Fuller test. Full details about the experimental protocol, study group, and time series extraction are provided in Javorka *et al* (2017).

The resulting time series were considered as realizations of the stochastic processes describing the dynamics of HP, SAP, and RESP: $\mathcal{H}=\{H_n\}$, $\mathcal{S}=\{S_n\}$, $\mathcal{R}=\{R_n\}$. An example of the signals, along with the respective time series, is reported in figure 2 panels A and B. The analyses were performed by setting $X=\mathcal{H}$ and $Y=\mathcal{S}$ for the CV system, while $X=\mathcal{H}$ and $Y=\mathcal{R}$ were considered for the CR system. The information terms $P_{X;Y}$, S_X, S_Y, $T_{X\rightarrow Y}$ and $T_{Y\rightarrow X}$ were computed as in equations (9)–(11), then the integration measures $\chi_{X;Y}$ and $\Phi_{X;Y}$ were derived as in equations (4) and (5).

2.2.2. Statistical and surrogate data analysis

To assess statistically significant differences across physiological states (REST, HUT and MA), a repeated measures ANOVA test was performed for each measure with a significance level of 5%. Given that the normality of within-subject differences was verified through the Kolmogorov–Smirnov test, to assess statistically significant changes between pairwise conditions (REST vs HUT, REST vs MA and HUT vs MA) the parametric paired Student's *t*-test with Bonferroni correction for multiple comparisons ($\alpha=0.05/3$) was performed.

To statistically validate the proposed measures, the surrogate data method (Theiler *et al* 1992) was employed to establish a significance level for each analyzed measure. Specifically, the statistical significance of $\chi_{X;Y}$, $\Phi_{X;Y}$, $T_{X\rightarrow Y}$ and $T_{Y\rightarrow X}$ was assessed using an iterative amplitude adjusted Fourier transform (IAAFT) algorithm (Schreiber and Schmitz 1996). Independent IAAFT surrogates were generated

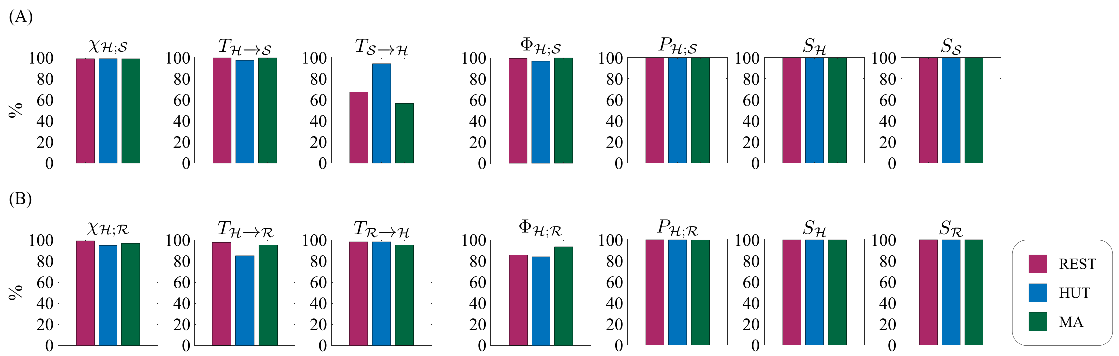

Figure 3. Barplots diplaying the percentage of subjects for whom the presence of CD integrated information $\chi_{X;Y}$ and its decomposition with $T_{X\to Y}$ and $T_{Y\to X}$, and WMS integrated information $\Phi_{X;Y}$ and its decomposition with $P_{X;Y}$, S_X and S_Y, was deemed as statistically significant, with regard to the cardiovascular (panel A) and cardiorespiratory (panel B) systems.

for each time series, preserving their individual linear autocorrelation structure and amplitude distribution while removing any cross-correlation between them. Conversely, the significance of $P_{X;Y}$, S_X, and S_Y was tested using random-shuffling surrogates (Theiler *et al* 1992), obtained by randomly permuting the temporal order of each series, thereby preserving the marginal distribution while destroying temporal dependencies under the null hypothesis of no dynamical structure. For each measure, the surrogate procedure was repeated 100 times to obtain a surrogate distribution. The original value was then compared with this distribution, using the 95*th* percentile as the significance threshold. Original values above this threshold were considered as statistically significant.

3. Results

This section reports the results obtained for the analysis of different integrated information measures performed on the beat-to-beat variability time series representative of the CV and CR dynamics at rest and under autonomic stressors.

Figures 4 and 5 present, respectively for CV and CR dynamics, the boxplot distributions and individual values of $\chi_{X;Y}$ and $\Phi_{X;Y}$, along with their constituent contributions, computed for the 127 subjects under the three experimental conditions (REST, HUT and MA), while figure 3 reports the percentage of subjects for whom the measures were deemed as statistically significant according to surrogate data analysis.

3.1. Integrated information of CV dynamics

The trends observed for the integration measures $\chi_{\mathcal{H};\mathcal{S}}$ and $\Phi_{\mathcal{H};\mathcal{S}}$, when considering the CV dynamics (figure 3(a)), reveal a statistically significant degree of integration. Specifically, for each measure, the percentages of subjects (out of 127) for whom statistical significance was detected according to surrogate data analysis (figure 3(a)) is close to 100% and appears largely unaffected by the task. An exception is observed for $T_{\mathcal{S}\to\mathcal{H}}$, which shows significance in approximately 50% of subjects during REST and MA.

Figure 4, panel A.1, reports no variations of $\chi_{\mathcal{H};\mathcal{S}}$ across the three conditions, with no statistically significant differences detected by the ANOVA test. In contrast, both TE components exhibit statistically significant differences across conditions: $T_{\mathcal{H}\to\mathcal{S}}$ shows a statistically significant decrease from REST to HUT and a significant increase from HUT to MA (figure 4, panel A.2), whereas $T_{\mathcal{S}\to\mathcal{H}}$ exhibits a statistically significant increase from REST to HUT, and a statistically significant decrease from HUT to MA (figure 4, panel A.3).

The WMS measure $\Phi_{\mathcal{H};\mathcal{S}}$ (figure 4, panel B.1) exhibits a different behavior, with statistically significant changes across conditions according to the ANOVA test. Post-hoc analysis reveals a statistically significant reduction from REST to HUT and a significant increase from HUT to MA. The three components of $\Phi_{\mathcal{H};\mathcal{S}}$, namely $P_{\mathcal{H};\mathcal{S}}$, $S_{\mathcal{H}}$, and $S_{\mathcal{S}}$ (figure 4, panels B.2–B.4), also show statistically significant modulation across conditions, but with an opposite trend: they increase from REST to HUT and decrease from HUT to MA. Additionally, $P_{\mathcal{H};\mathcal{S}}$ and $S_{\mathcal{S}}$ display a significant decrease from REST to MA according to the Student's *t*-test.

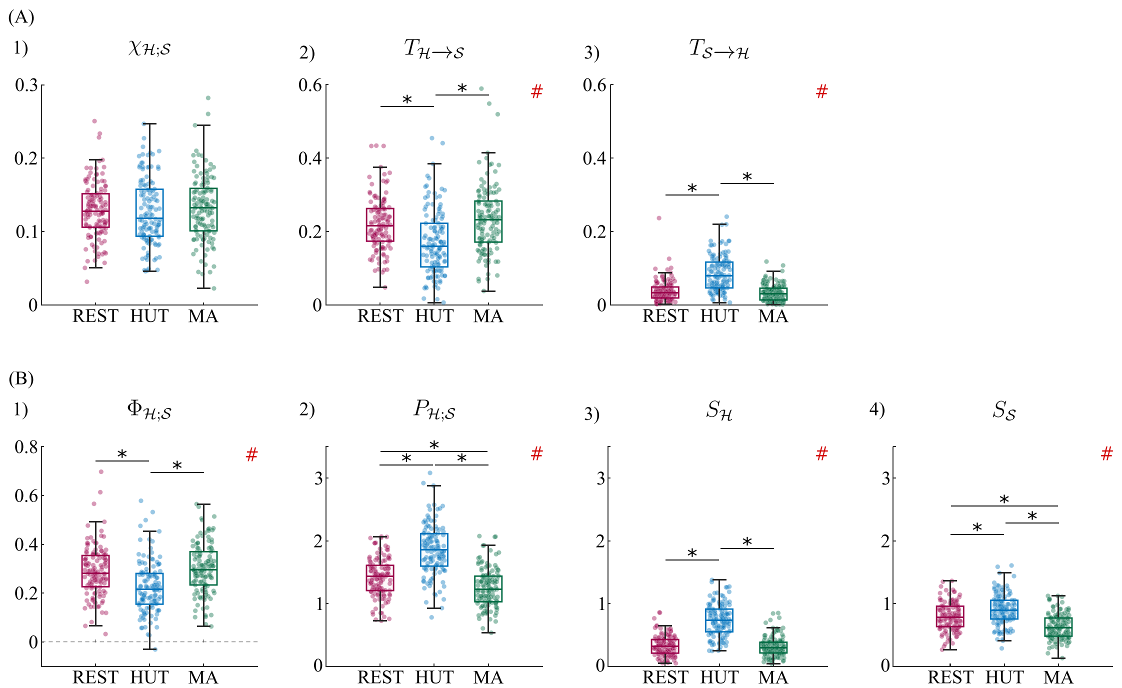

Figure 4. Boxplot distributions and individual values of: (A) $\chi_{\mathcal{H};\mathcal{S}}$ (subpanel 1) and its decomposition with $T_{\mathcal{H}\to\mathcal{S}}$ and $T_{\mathcal{S}\to\mathcal{H}}$(subpanels 2 and 3), and (B) $\Phi_{\mathcal{H};\mathcal{S}}$ (subpanel 1) and its decomposition with $P_{\mathcal{H};\mathcal{S}}$, $S_{\mathcal{H}}$ and $S_{\mathcal{S}}$ (subpanels 2, 3 and 4), for the cardiovascular system. $\#p < 0.05$, ANOVA; $*p < 0.05/3$ paired t-test.

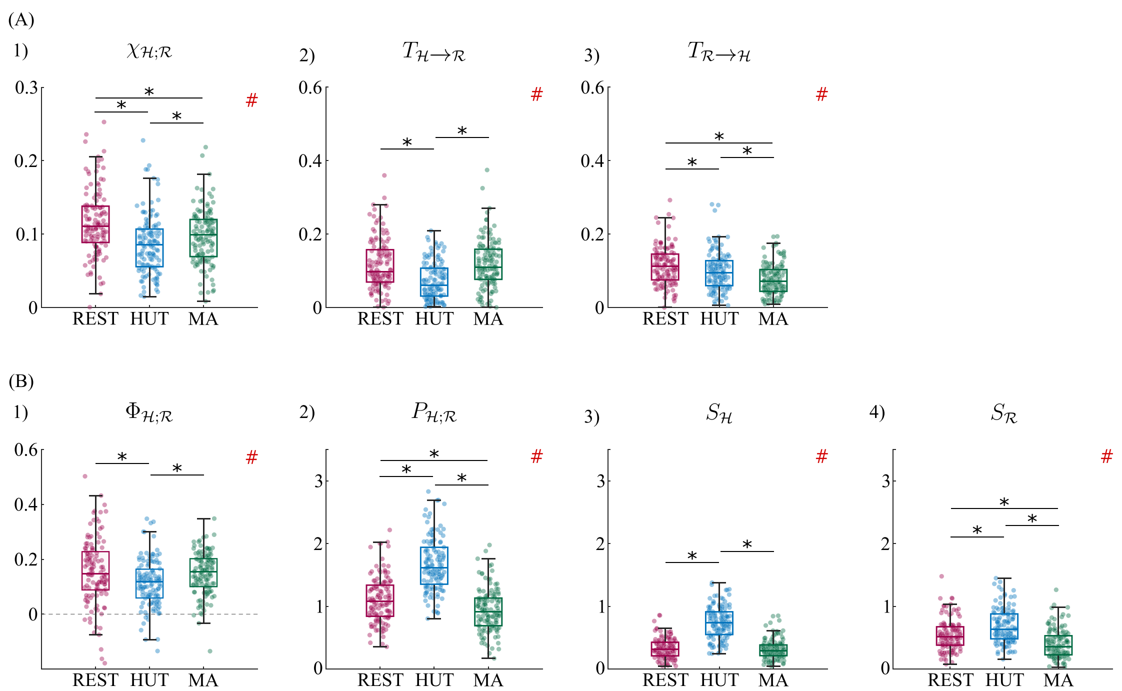

Figure 5. Boxplot distributions and individual values of: (A) $\chi_{\mathcal{H};\mathcal{R}}$ (subpanel 1) and its decomposition with $T_{\mathcal{H}\to\mathcal{R}}$ and $T_{\mathcal{R}\to\mathcal{H}}$(subpanels 2 and 3), and (B) $\Phi_{\mathcal{H};\mathcal{R}}$ (subpanel 1) and its decomposition with $P_{\mathcal{H};\mathcal{R}}$, $S_{\mathcal{H}}$ and $S_{\mathcal{R}}$ (subpanels 2, 3 and 4) for the cardiorespiratory system. $\#p < 0.05$, ANOVA; $*p < 0.05/3$ paired t-test.

3.2. Integrated information of CR dynamics

The analysis of the integration measures $\chi_{\mathcal{H};\mathcal{R}}$ and $\Phi_{\mathcal{H};\mathcal{R}}$ for the CR dynamics (figure 3(b)) reveals that all information measures report almost 100% of statistical significance across conditions; exceptions are observed for $T_{\mathcal{H}\to\mathcal{R}}$ during HUT and for $\Phi_{\mathcal{H};\mathcal{R}}$ during REST and HUT, where significance is detected in approximately 80% of subjects. Figure 5, panel A, denotes a clear stress-induced modulation affecting both the integration measures and their constituent information terms, which is statistically significant according to the ANOVA test. A statistically significant modulation of $\chi_{\mathcal{H};\mathcal{R}}$ is observed across conditions (figure 5, panel A.1), with a significant decrease from REST to HUT and from REST to MA, and a significant increase from HUT to MA. Both TE components also show statistically significant differences (figure 5, panels A.2-A.3). In particular, $T_{\mathcal{R}\to\mathcal{H}}$ exhibits a progressive decrease from REST to HUT and from HUT to MA, resulting also in an overall reduction from REST to MA (panel A.3), whereas $T_{\mathcal{H}\to\mathcal{R}}$ shows a statistically significant decrease from REST to HUT and a significant increase from HUT to MA (panel A.2).

Conversely, $\Phi_{\mathcal{H};\mathcal{R}}$ (figure 5 panel B.1) displays a statistically significant reduction from REST to HUT and a significant increase from HUT to MA, with no differences between REST and MA. Its components, $P_{\mathcal{H};\mathcal{R}}$, $S_{\mathcal{H}}$ and $S_{\mathcal{R}}$ (figure 5, panels B.2-B.4), show a significant increase from REST to HUT followed by a significant decrease from HUT to MA; moreover, $P_{\mathcal{H};\mathcal{R}}$ and $S_{\mathcal{R}}$ decrease significantly from REST to MA. The stronger concomitant increase in $S_{\mathcal{H}}$ and $S_{\mathcal{R}}$ with respect to the increase of $P_{\mathcal{H};\mathcal{R}}$ during HUT results in a net reduction of $\Phi_{\mathcal{H};\mathcal{R}}$, whereas during MA the opposing variations balance each other, leaving $\Phi_{\mathcal{H};\mathcal{R}}$ unchanged. Notably, $\Phi_{\mathcal{H};\mathcal{R}}$ can assume negative values, as shown in figure 5, panel B.1.

4. Discussion

In this study, we employed two different measures of dynamical complexity, namely, the CD and the WMS integrated information, to characterize the modulation of integration in CV and CR systems across different physiological states (rest, postural and mental stress). While CD operationalizes integration in terms of directed information transfer among system components, reflecting the extent of causal interactivity, WMS quantifies the degree to which the system, considered as a whole, generates PI beyond that accounted for by its parts independently. Together, these measures capture complementary aspects of the balance between integration and differentiation in physiological dynamics.

The use of integrated information measures, together with the analysis of their constituent components, enabled a more refined characterization of the statistical dependencies underlying CV and CR dynamics. The main findings discussed in sections 4.1 and 4.2, can be summarized as follows: (i) both CV and CR systems exhibit significant dynamical integration at rest and during physiological stress; (ii) postural stress induces a reduction of integration in both systems, particularly evident in the $\Phi_{X;Y}$ measure; (iii) during mental stress the reduction of integration is less pronounced and emerges only in the CR dynamics as captured by $\chi_{X;Y}$; (iv) the decomposition of the integrated information measures into transfer- and storage-related components is consistent with established physiological responses, including increased regularity of oscillations during postural stress, enhanced information transfer from $\mathcal{S}$ to $\mathcal{H}$ under postural stress, and reduced transfer from $\mathcal{R}$ to $\mathcal{H}$ during both postural and mental stress.

4.1. Integration of CV dynamics

The integration of CV dynamics was supported by the statistically significant values of both integrated information measures, $\chi_{\mathcal{H};\mathcal{S}}$ and $\Phi_{\mathcal{H};\mathcal{S}}$, across all experimental conditions. However, the two measures exhibited different sensitivities: while $\chi_{\mathcal{H};\mathcal{S}}$ remained largely unchanged across conditions, $\Phi_{\mathcal{H};\mathcal{S}}$ showed a marked reduction during postural stress. These differences can be interpreted by examining the information-theoretic components underlying each measure.

The absence of statistically significant differences in $\chi_{\mathcal{H};\mathcal{S}}$ values across conditions reflects the opposite trends reported for the two TE terms, $T_{\mathcal{H}\to\mathcal{S}}$ and $T_{\mathcal{S}\to\mathcal{H}}$. Previous studies documented an increase in the TE from SAP to HP during the orthostatic stress, due to a dominance of high pressure baroreflex mechanism in HP variability resulting in an often observed decreased HP oscillations complexity (Barà *et al* 2023), and a decrease in TE from HP to SAP, resulting in a overall reduced causal coupling (Javorka *et al* 2017). The results are consistent with the physiological mechanisms described in previous works on CV variability analysis (Porta *et al* 2011, Javorka *et al* 2018). Indeed, it is well-known that HP and SAP are likely to interact in a closed-loop, according to the existence of baroreflex mechanisms, acting from SAP to HP, and of the mechanical feedforward mechanisms, acting from HP to SAP (Javorka *et al* 2018). Postural stress has been proven to induce an alteration on the closed-loop CV interaction, as a consequence of the tilt-induced activation of the baroreflex feedback, accompanied by a weakening of the mechanical feedforward interconnections (Mullen *et al* 1997, Nollo *et al* 2005). This explains why the integration of CV dynamics, measured in terms of CD, remains unaffected by postural stress, despite evidence of task-induced responses in its components. Moreover, the integration of CV dynamics remained largely unaltered also during mental stress. This is in accordance with previous studies indicating that MA task does not induce significant alterations in the strength and delay of CV interactions (Javorka et al 2017). Indeed, whilst the autonomic nervous system plays a crucial role in the CV system's adaptation to mental stress (Sant'anna et al 2003), the alterations induced are intricate and subject to inter-individual variability and the changes are not dominantly mediated by alterations in baroreflex function (Javorka et al 2017). This makes the detection of statistically significant differences in the interactions between HP and SAP more challenging.

On the contrary, a significant modulation of CV integration across conditions was detected using $\Phi_{\mathcal{H};\mathcal{S}}$, particularly during HUT, where a marked reduction compared to REST was observed. The increase in PI ($P_{\mathcal{H};\mathcal{S}}$) observed during postural stress reflects enhanced system predictability, consistent with strengthened internal CV dynamics and increased redundant cooperation within the system (Faes et al 2017). Previous studies have also reported greater regularity in HP and SAP dynamics during HUT, which in the present framework is reflected by the increase in $S_{\mathcal{H}}$ and $S_{\mathcal{S}}$ (Porta et al 2000, Javorka et al 2018). Physiologically, these modulations occurring during HUT, can be associated with the increase of the vagal withdrawal and to the sympathetic activation, due to the reduction of venous return leading to the baroreceptor unloading (Cooke et al 1999, Javorka et al 2017). The different response to HUT of the WMS measure compared to the CD measure can be explained either by the different concepts underlying the two measures (difference in self and joint predictability vs exchange of information) or by the bias towards lower/negative values inherent in the WMS measure; the latter interpretation is supported by studies showing increased redundancy of CV interactions during postural stress (Krohova et al 2019).

During MA, both $P_{\mathcal{H};\mathcal{S}}$ and $S_{\mathcal{S}}$ showed a significant decrease, indicating a reduction in CV interaction. This effect may be related to the decreased regularity of SAP dynamics (Javorka et al 2018), possibly reflecting cortical central commands modulating vascular resistance via sympathetic pathways (Fauvel et al 2000). In contrast, $S_{\mathcal{H}}$ appears largely unaffected by mental stress, in agreement with previous findings (Widjaja et al 2015, Faes et al 2016).

4.2. Integration of CR dynamics

Integrated information analysis of CR dynamics revealed significant integration at rest, followed by a reduction during postural stress, as detected by both $\chi_{\mathcal{H};\mathcal{R}}$ and $\Phi_{\mathcal{H};\mathcal{R}}$, and during mental stress, as captured by $\chi_{\mathcal{H};\mathcal{R}}$ only. The decrease in $\chi_{\mathcal{H};\mathcal{R}}$ during HUT reflects the reduction in both TE components ($T_{\mathcal{R}\to\mathcal{H}}$ and $T_{\mathcal{H}\to\mathcal{R}}$), consistent with sympathetic predominance and attenuation of RSA (Cooke et al 1999, Faes et al 2014). In contrast, during mental stress $T_{\mathcal{H}\to\mathcal{R}}$ partially recovers whereas $T_{\mathcal{R}\to\mathcal{H}}$ remains reduced, in agreement with previous evidence of vagal inhibition and weakened CR coupling (Porta et al 2012, Krohova et al 2019).

A similar pattern in CR integration was observed for $\Phi_{\mathcal{H};\mathcal{R}}$, which showed a significant decrease during HUT. This behavior can be interpreted by examining its components, $P_{\mathcal{H};\mathcal{R}}$, $S_{\mathcal{H}}$, and $S_{\mathcal{R}}$. The increase in $P_{\mathcal{H};\mathcal{R}}$ during postural stress indicates enhanced predictability of CR dynamics, consistent with stronger internal dynamics and increased redundant cooperation (Faes et al 2025). Previous studies have also reported reduced respiratory complexity during HUT (Pinto et al 2023), typically associated with increased tidal volume and/or decreased breathing rate. During mental stress, the observed reduction in CR coupling may be attributed to vagal withdrawal and attenuation of RSA (Faes et al 2016), together with decreased respiratory regularity (Valente et al 2018, Zanetti et al 2019). Overall, postural stress induced a clear reduction in CR integration, whereas mental stress showed a weaker effect, reaching statistical significance only when assessed using $\chi_{\mathcal{H};\mathcal{R}}$.

4.3. Methodological remarks and limitations

From a methodological perspective, CD is closely related to the Mutual Information Rate (MIR), a well-established information-theoretic measure that quantifies the dynamic interdependence between pairs of stochastic processes (Duncan 1970). MIR can be expressed in terms of entropy rates or conditional mutual information and captures both the intrinsic dynamics of individual processes and their interactions (Barà et al 2023). Similar to CD, MIR can be decomposed into two TE components plus an additional term reflecting zero-lag mutual information between X and Y, commonly referred to as the instantaneous term. Although the instantaneous information term may carry meaningful physiological interpretations, it is not included in the definition of CD. For instance, the instantaneous information shared between HP and SAP has been shown to decrease significantly during HUT (Barà et al 2023), whereas weak instantaneous interactions between HP and RESP were observed both at REST and during HUT (Pinto et al 2023). Like most measures of integrated information, the CD accounts only for lagged interactions, and, as such, it may not fully capture system integration in physiological systems, where meaningful coupling occurs also without delays, such as in the case of CV and CR dynamics, where zero-lag effects can be prominent (Faes et al 2013). These considerations suggest that future integration measures should explicitly account for the instantaneous component.

Another important aspect emerging from the analysis of WMS is that this measure can, in certain cases, assume negative values. As illustrated in figure 1(c), the regions highlighted in azure correspond to information that is subtracted in the WMS formulation. In particular, they include information that is already accounted for by the individual parts when considered separately. When this redundant contribution is large, meaning that most of the PI of the whole system is already explained by its parts, the subtraction can dominate, causing WMS to take negative values. This interpretation becomes formally clear within the integrated information decomposition (ΦID) framework (Mediano *et al* 2019), where WMS is shown to include the double-redundancy information atom with a negative sign in the lattice representation. Since non-negativity is generally regarded as a fundamental requirement for a measure of integrated information, this feature represents a conceptual limitation. A possible solution, proposed in Mediano *et al* (2025), consists in adding back the subtracted redundancy term, thereby ensuring that the resulting measure is always non-negative. Therefore, a future implementation of the framework should explore the impact of this recently proposed correction to the WMS formulation to ensure non-negativity.

Moreover, another important remark is that a linear VAR-based approach is most appropriate when the underlying processes can be reasonably assumed to be stationary and approximately linear, assumptions that may not hold under various physiological conditions, instead characterized by strongly nonlinear dynamics. Nevertheless, previous studies have demonstrated that VAR models may in principle be able to describe also the dynamics of processes with nonlinear generating mechanisms, even if at the cost of increasing considerably (theoretically up to infinite) the model order (Hannan 1979, Faes *et al* 2025, Sparacino *et al* 2025). However, since fitting a finite-order VAR model to processes characterized by strongly nonlinear dynamics may fail to suitably reflect some kinds of dynamic dependencies, a future extension should envisage the realization of a model-free version of the framework, starting from already implemented TE and PI measures (Faes *et al* 2015, Barà *et al* 2023, Saputo *et al* 2026). Such a model-free version would be able to fully account for nonlinear physiological dynamics, but should face theoretical and practical challenges posed by estimation (e.g. curse of dimensionality) (Vlachos and Kugiumtzis 2010, Pinto *et al* 2024).

4.4. Potential clinical and translational applications

The proposed measures appear capable of capturing changes in autonomic regulation, as evidenced by the significant differences observed between resting and tilt conditions, highlighting their potential clinical relevance. The statistically significant variations reported during baroreflex activation allow us to expect that the measures will be as well sensitive to syncope-related responses, given the well-established association between syncope events and alterations in baroreflex regulation (Folino *et al* 2007). Furthermore, recent studies have demonstrated the capability of information-theoretic approaches to better characterize an impact of aging in CV autonomic regulation (Takahashi *et al* 2012, Catai *et al* 2014), and to identify CV alterations in pathological conditions, e.g. in patients with autonomic dysregulation, including patients with diabetes mellitus, neurological disorders or after acute myocardial infarction (Nollo *et al* 2002, Moura-Tonello *et al* 2014, Botchway *et al* 2026). Thus, we can assume that metrics of integrated information may contribute to the assessment of further pathophysiological conditions (e.g. other stressors, aging, heart failure, and syncope), even if their clinical potential and translational implications remain to be systematically investigated and validated in future studies.

Further analyses should be also conducted to investigate the potential effect of sex on dynamical integration, since several studies have demonstrated sex–related differences in CV function (Shoemaker *et al* 2001, Joyner *et al* 2015, Ontivero-Ortega *et al* 2025).

5. Conclusion

This study investigated the concept of dynamical integration in CV and CR systems at different physiological conditions using two IIT framework-based measures, i.e. CD and WMS.

Our findings demonstrate that both systems exhibit significant dynamical integration at rest, which is systematically modulated by physiological challenges represented by postural challenge and cognitive load. In particular, orthostatic stress markedly reduces integration in both systems, reflecting a weakening of coordinated interactions between their components. Mental stress, in contrast, evidences more selective and measure-dependent effects. The obtained results suggest that CD and WMS capture complementary aspects of information dynamics, highlighting that integration is not a single, well-defined concept, but instead depends on the specific information-theoretic principle used for its quantification.

Overall, our study suggests that a deeper understanding of how integration emerges across levels of physiological organization may provide novel insights into the functional architecture of autonomic control, even if caution is warranted when interpreting integration measures in complex physiological dynamics given their methodological limitations.

Acknowledgments

This research activity was supported by PRIN 2022 project 'HONEST' (funded by MUR, code 2022YMHNPY, CUP B53D23003020006). I.F. Ph.D. scholarship was funded by Regione Siciliana—Call no. 15/2024 - PR Sicilia FSE+ 2021-2027. R.S. Ph.D. scholarship was funded by the project 'DARE—Digital lifelong pRevEntion initiative' (MUR, PNC D.D. 931 06/06/2022, code PNC0000002). M.J. was funded by Grant VEGA No.1/0107/25.

Data availability statement

The data that support the findings of this study are available upon reasonable request from the authors.

Conflict of interest

The authors declare there is no conflict of interest associated with this research or the writing of this paper.

Author contributions

Irene Franzone 0009-0004-8489-2487
Conceptualization (equal), Data curation (equal), Formal analysis (equal), Software (equal), Validation (equal), Visualization (equal), Writing – original draft (equal)

Roberta Saputo 0009-0007-2750-5374
Data curation (equal), Methodology (equal), Software (equal)

Yuri Antonacci 0000-0002-6956-6323
Methodology (equal), Software (equal), Supervision (equal), Writing – review & editing (equal)

Michal Javorka 0000-0001-7562-5193
Data curation (equal), Writing – review & editing (equal)

Riccardo Pernice 0000-0002-9992-3221
Investigation (equal), Methodology (equal), Project administration (equal), Supervision (equal), Writing – review & editing (equal)

Luca Faes 0000-0002-3271-5348
Conceptualization (equal), Funding acquisition (equal), Investigation (equal), Methodology (equal), Project administration (equal), Resources (equal), Software (equal), Supervision (equal), Validation (equal), Writing – review & editing (equal)

References

Balduzzi D and Tononi G 2008 Integrated information in discrete dynamical systems: motivation and theoretical framework *Comput. Biol.* **4** e1000091

Barà C, Sparacino L, Pernice R, Antonacci Y, Porta A, Kugiumtzis D and Faes L 2023 Comparison of discretization strategies for the model-free information-theoretic assessment of short-term physiological interactions *Chaos* **33** 033127

Barnett L, Barrett A B and Seth A K 2009 Granger causality and transfer entropy are equivalent for Gaussian variables *Phys. Rev. Lett.* **103** 238701

Barrett A B, Barnett L and Seth A K 2010 Multivariate Granger causality and generalized variance *Phys. Rev. E* **81** 041907

Barrett A B and Seth A K 2011 Practical measures of integrated information for time-series data *Comput. Biol.* **7** e1001052

Bialek W, Nemenman I and Tishby N 2001 Predictability, complexity and learning *Neural Comput.* **13** 2409–63

Botchway B O A *et al* 2026 From brain waves to heartbeats: exploring the combined role of electroencephalography and heart-rate variability in Alzheimer's disease diagnosis and management *J. Alzheimer's Dis.* **111** 5–31

Catai A M, Takahashi A C, Perseguini N M, Milan J C, Minatel V, Rehder-Santos P, Marchi A, Bari V and Porta A 2014 Effect of the postural challenge on the dependence of the cardiovascular control complexity on age *Entropy* **16** 6686–704

Cohen M A and Taylor J A 2002 Short-term cardiovascular oscillations in man: measuring and modelling the physiologies *J. Physiol.* **542** 669–83

Cooke W H, Hoag J B, Crossman A A, Kuusela T A, Tahvanainen K U and Eckberg D L 1999 Human responses to upright tilt: a window on central autonomic integration *J. Physiol.* **517** 617–28

Cover T M 1999 *Elements of Information Theory* (Wiley)

Duncan T E 1970 On the calculation of mutual information *SIAM J. Appl. Math.* **19** 215–20

Eckberg D L 2003 Topical review: the human respiratory gate *J. Physiol.* **548** 339–52

Faes L, Erla S, Porta A and Nollo G 2013 A framework for assessing frequency domain causality in physiological time series with instantaneous effects *Phil. Trans. R. Soc. A* **371** 1997

Faes L, Kugiumtzis D, Nollo G, Jurysta F and Marinazzo D 2015 Estimating the decomposition of predictive information in multivariate systems *Phys. Rev. E* **91** 032904

Faes L, Marinazzo D, Montalto A and Nollo G 2014 Lag-specific transfer entropy as a tool to assess cardiovascular and cardiorespiratory information transfer *IEEE Trans. Biomed. Eng.* **61** 2556–68

Faes L, Mijatovic G, Sparacino L and Porta A 2025 Predictive information decomposition as a tool to quantify emergent dynamical behaviors in physiological networks *IEEE Trans. Biomed. Eng.* **72** 3515–24

Faes L, Nollo G and Porta A 2017 Information Decomposition: A Tool to Dissect Cardiovascular and Cardiorespiratory Complexity *Complexity and Nonlinearity in Cardiovascular Signals* (Springer) pp 87–113

Faes L, Porta A, Nollo G and Javorka M 2016 Information decomposition in multivariate systems: definitions, implementation and application to cardiovascular networks *Entropy* **19** 5

Fauvel J P, Cerutti C, Quelin P, Laville M, Gustin M P, Paultre C Z and Ducher M 2000 Mental stress–induced increase in blood pressure is not related to baroreflex sensitivity in middle-aged healthy men *Hypertension* **35** 887–91

Folino A F, Russo G, Porta A, Buja G, Cerutti S and Iliceto S 2007 Modulations of autonomic activity leading to tilt-mediated syncope *Int. J. Cardiol.* **120** 102–7

Galletly D and Larsen P 1998 Relationship between cardioventilatory coupling and respiratory sinus arrhythmia *Br. J. Anaesth.* **80** 164–8

Hannan E J 1979 The Statistical Theory of Linear Systems *Developments in Statistics* vol 2 (Elsevier) pp 83–121

Hunter P and Nielsen P 2005 A strategy for integrative computational physiology *Physiology* **20** 316–25

Ivanov P C 2021 The new field of network physiology: building the human physiolome

Javorka M, Krohova J, Czippelova B, Turianikova Z, Lazarova Z, Javorka K and Faes L 2017 Basic cardiovascular variability signals: mutual directed interactions explored in the information domain *Physiol. Meas.* **38** 877

Javorka M, Krohova J, Czippelova B, Turianikova Z, Lazarova Z, Wiszt R and Faes L 2018 Towards understanding the complexity of cardiovascular oscillations: insights from information theory *Comput. Biol. Med.* **98** 48–57

Joyner M J, Barnes J N, Hart E C, Wallin B G and Charkoudian N 2015 Neural control of the circulation: how sex and age differences interact in humans *Compr. Physiol.* **5** 193–215

Krohova J, Faes L, Czippelova B, Turianikova Z, Mazgutova N, Pernice R, Busacca A, Marinazzo D, Stramaglia S and Javorka M 2019 Multiscale information decomposition dissects control mechanisms of heart rate variability at rest and during physiological stress *Entropy* **21** 526

Lizier J T, Prokopenko M and Zomaya A Y 2014 A Framework for the Local Information Dynamics of Distributed Computation in Complex Systems *Guided Self-Organization: Inception* (Springer) pp 115–58

Lütkepohl H 2013 *Introduction to Multiple Time Series Analysis* (Springer)

Mediano P A, Rosas F E, Bor D, Seth A K and Barrett A B 2022 The strength of weak integrated information theory *Trends Cogn. Sci.* **26** 646–55

Mediano P A, Rosas F E, Farah J C, Shanahan M, Bor D and Barrett A B 2022 Integrated information as a common signature of dynamical and information-processing complexity *Chaos* **32** 013115

Mediano P A, Rosas F E, Luppi A I, Carhart-Harris R L, Bor D, Seth A K and Barrett A B 2025 Toward a unified taxonomy of information dynamics via integrated information decomposition *Proc. Natl Acad. Sci.* **122** e2423297122

Mediano P A, Rosas F, Carhart-Harris R L, Seth A K and Barrett A B 2019 Beyond integrated information: a taxonomy of information dynamics phenomena (arXiv:1909.02297)

Mediano P A, Seth A K and Barrett A B 2018 Measuring integrated information: comparison of candidate measures in theory and simulation *Entropy* **21** 17

Mijatovic G, Antonacci Y, Javorka M, Marinazzo D, Stramaglia S and Faes L 2025 Network representation of higher-order interactions based on information dynamics *IEEE Trans. Netw. Sci. Eng.* **12** 1872–84

Moura-Tonello S C, Takahashi A C, Francisco C O, Lopes S L, Del Vale A M, Borghi-Silva A, Leal A M, Montano N, Porta A and Catai A M 2014 Influence of type 2 diabetes on symbolic analysis and complexity of heart rate variability in men *Diabetol. Metab. Syndr.* **6** 13

Mullen T J, Appel M L, Mukkamala R, Mathias J M and Cohen R J 1997 System identification of closed-loop cardiovascular control: effects of posture and autonomic blockade *Am. J. Physiol.-Heart Circ. Physiol.* **272** H448–61

Nollo G, Faes L, Porta A, Antolini R and Ravelli F 2005 Exploring directionality in spontaneous heart period and systolic pressure variability interactions in humans: implications in the evaluation of baroreflex gain *Am. J. Physiol.-Heart Circ. Physiol.* **288** H1777–85

Nollo G, Faes L, Porta A, Pellegrini B, Ravelli F, Del Greco M, Disertori M and Antolini R 2002 Evidence of unbalanced regulatory mechanism of heart rate and systolic pressure after acute myocardial infarction *Am. J. Physiol.-Heart Circ. Physiol.* **283** H1200–7

Oizumi M, Amari S-i, Yanagawa T, Fujii N and Tsuchiya N 2016 Measuring integrated information from the decoding perspective *Comput. Biol.* **12** e1004654

Oizumi M, Tsuchiya N and Amari S-i 2016 Unified framework for information integration based on information geometry *Proc. Natl Acad. Sci.* **113** 14817–22

Ontivero-Ortega M, Iovino M, Pernice R, Barà C, Javorka M, Faes L and Stramaglia S 2025 Assessment of sex-related differences in cardiovascular control using high-order feature importance *Eur. Phys. J. Spec. Top.* 1–12

Pan J and Tompkins W J 2007 A real-time QRS detection algorithm *IEEE Trans. Biomed. Eng.* **3** 230–6

Pinto H, Antonacci Y, Pernice R, Barà C, Javorka M, Faes L and Rocha A P 2023 Decomposing the mutual information rate of heart period and respiration variability series to assess cardiorespiratory interactions *2023 45th Annual Int. Conf. IEEE Engineering in Medicine & Biology Society (EMBC)* (IEEE) pp 1–4

Pinto H, Lazic I, Antonacci Y, Pernice R, Gu D, Barà C, Faes L and Rocha A P 2024 Testing dynamic correlations and nonlinearity in bivariate time series through information measures and surrogate data analysis *Front. Netw. Physiol.* **4** 1385421

Pompe B, Blidh P, Hoyer D and Eiselt M 1998 Using mutual information to measure coupling in the cardiorespiratory system *IEEE Eng. Med. Biol. Mag.* **17** 32–39

Porta A, Bassani T, Bari V, Tobaldini E, Takahashi A C, Catai A M and Montano N 2012 Model-based assessment of baroreflex and cardiopulmonary couplings during graded head-up tilt *Comput. Biol. Med.* **42** 298–305

Porta A, Catai A M, Takahashi A C, Magagnin V, Bassani T, Tobaldini E, Van De Borne P and Montano N 2011 Causal relationships between heart period and systolic arterial pressure during graded head-up tilt *Am. J. Physiol.-Regul. Integr. Comp. Physiol.* **300** R378–86

Porta A, Guzzetti S, Montano N, Pagani M, Somers V, Malliani A, Baselli G and Cerutti S 2000 Information domain analysis of cardiovascular variability signals: evaluation of regularity, synchronisation and co-ordination *Med. Biol. Eng. Comput. Physiol.* **38** 180–8

Rosenblum M G, Kurths J, Pikovsky A, Schafer C, Tass P and Abel H-H 1998 Synchronization in noisy systems and cardiorespiratory interaction *IEEE Eng. Med. Biol. Mag.* **17** 46–53

Sant'anna I D, de Sousa E B, de Moraes A V, Loures D L, Mesquita E T and da Nóbrega A C L 2003 Cardiac function during mental stress: cholinergic modulation with pyridostigmine in healthy subjects *Clin. Sci.* **105** 161–5

Saputo R, Barà C, Franzone I, Javorka M, Pernice R and Faes L 2026 Partial decomposition of information dynamics elicits unique and shared modes of cardiovascular and cardiorespiratory control in response to autonomic stressors *Eur. Phys. J. Spec. Top.* 1–21

Schreiber T 2000 Measuring information transfer *Phys. Rev. Lett.* **85** 461

Schreiber T and Schmitz A 1996 Improved surrogate data for nonlinearity tests *Phys. Rev. Lett.* **77** 635

Schulz S, Adochiei F-C, Edu I-R, Schroeder R, Costin H, Bär K-J and Voss A 2013 Cardiovascular and cardiorespiratory coupling analyses: a review *Phil. Trans. R. Soc. A* **371** 20120191

Schwarz G 1978 Estimating the dimension of a model *Ann. Stat.* **6** 461–4

Seth A K, Barrett A B and Barnett L 2011 Causal density and integrated information as measures of conscious level *Phil. Trans. R. Soc.* **369** 3748–67

Shaffer F and Ginsberg J P 2017 An overview of heart rate variability metrics and norms *Public Health* **5** 258

Shoemaker J K, Hogeman C S, Khan M, Kimmerly D S and Sinoway L I 2001 Gender affects sympathetic and hemodynamic response to postural stress *Am. J. Physiol.-Heart Circ. Physiol.* **281** H2028–35

Sparacino L, Mijatovic G, Antonacci Y, Ricci L, Marinazzo D, Stramaglia S and Faes L 2025 Decomposing multivariate information rates in networks of random processes *Phys. Rev. E* **112** 044313

Takahashi A C, Porta A, Melo R C, Quitério R J, da Silva E, Borghi-Silva A, Tobaldini E, Montano N and Catai A M 2012 Aging reduces complexity of heart rate variability assessed by conditional entropy and symbolic analysis *Intern. Emerg. Med.* **7** 229–35

Theiler J, Eubank S, Longtin A, Galdrikian B and Farmer J D 1992 Testing for nonlinearity in time series: the method of surrogate data *Physica D* **58** 77–94

Tononi G 2012 Integrated information theory of consciousness: an updated account *Arch. Ital. Biol.* **150** 56–90

Tononi G and Koch C 2015 Consciousness: here, there and everywhere? *Phil. Trans. R. Soc. B* **370** 20140167

Valente M, Javorka M, Porta A, Bari V, Krohova J, Czippelova B, Turianikova Z, Nollo G and Faes L 2018 Univariate and multivariate conditional entropy measures for the characterization of short-term cardiovascular complexity under physiological stress *Physiol. Meas.* **39** 014002

Vlachos I and Kugiumtzis D 2010 Nonuniform state-space reconstruction and coupling detection *Phys. Rev. E–Stat. Nonlinear and Soft Matter Phys.* **82** 016207

Widjaja D, Montalto A, Vlemincx E, Marinazzo D, Van Huffel S and Faes L 2015 Cardiorespiratory information dynamics during mental arithmetic and sustained attention *PLoS One* **10** e0129112

Zanetti M, Faes L, Nollo G, De Cecco M, Pernice R, Maule L, Pertile M and Fornaser A 2019 Information dynamics of the brain, cardiovascular and respiratory network during different levels of mental stress *Entropy* **21** 275